Macromolecules
ARTICLE

Macromolecules **2009**, *42*, 7797–7810 **7797**
DOI: 10.1021/ma901406t

Microkinetic Modeling of Structural Properties of Poly(vinyl chloride)

Joris Wieme, Marie-Françoise Reyniers,* and Guy B. Marin

Laboratory for Chemical Technology, Ghent University Krijgslaan 281 (S5), B-9000 Gent, Belgium

Received June 30, 2009; Revised Manuscript Received September 15, 2009

ABSTRACT: The free radical suspension polymerization of vinyl chloride is modeled at the elementary reaction level, systematically taking into account diffusion limitations. By deriving balances for structurally distinct polymer and radical species the formation of structural defects can be followed: monomer conversion, averages of the molar mass distribution and the structural defects content can be calculated as a function of polymerization time for industrially relevant conditions. A good agreement between literature reported and calculated values for these properties is obtained for a polymerization temperature range of 325−340 K, a dicetyl peroxydicarbonate and dimyristyl peroxydicarbonate initiator concentration range of 0.00069−1.0 wt %, and a monomer conversion range of 12−96%. The increase of the branching content and the decrease of the terminal double bond content at high monomer conversions can be explained in terms of a favoring of monomolecular reactions and the increasing importance of addition reactions to unsaturations at these conditions.

1. Introduction

Poly(vinyl chloride) (PVC) is, by volume, one of the largest thermoplastics manufactured in the world. Despite its importance, poly(vinyl chloride) also poses many challenges. During processing, storage and utilization, PVC degrades as it is exposed to high temperatures, high mechanical stresses, or ultraviolet light. Degradation of the polymer occurs by successive elimination of hydrogen chloride yielding long polyenes which are consequently causing discoloration, deterioration of the mechanical properties, and a lowering of the chemical resistance.

Since the thermal stability of PVC is much lower than can be expected on the basis of its regular structure, several research groups have studied this matter.[1−10] The main conclusion of these studies is that a decrease of the thermal stability is related to the presence of specific irregularities, so-called defects, in the structure of the polymer. The chlorine atoms contained in some of these irregular structures tend to eliminate easily at higher temperatures, thereby creating initiation sites for the degradation process.[11]

The most labile structural defects are internal allylic and tertiary chlorine functional groups, viz. Figure 1. Indeed, the bond dissociation energy (BDE) of carbon-chlorine bonds involving an allylic or tertiary chlorine is remarkably lower than that of a regular carbon-chlorine bond in PVC, as can be seen from Table 1. Since these bonds are the weakest bonds present in the PVC chain, they will first break upon heating and, hence, initiate thermal degradation reactions. In the absence of defects, the polymer would be stable up to at least 473 K. However, because of the presence of structural defects, commercially available PVC already degrades at temperatures as low as 393 K in the absence of stabilizers, a temperature that is easily surpassed when processing the polymer.

Producers of polymers in general and of poly(vinyl chloride) in particular, strive for certain desirable customer properties such as tensile strength, glass transition temperature, thermal stability, processability, etc. These in turn are controlled by fundamental molecular and morphological properties of the polymer product such as molar mass distribution (MMD), structural defects content, particle size distribution (PSD), etc. Considering the great industrial importance of free radical polymerization processes, it is crucial to develop fundamental models linking polymer properties to the applied polymerization conditions such as temperature and amount and type of initiator. This would allow for the optimization of existing processes and the development of new processes, but also for the investigation of the conditions favoring the formation of the structural defects.

Vinyl chloride (VC) suspension polymerization has been modeled by several groups, most recently by those of Xie et al.,[14,15] Kiparissides et al.,[16] Talamini et al.,[17,18] De Roo et al.,[19,20] Krallis et al.,[21] and Wieme et al.[22] All mentioned models make use of the so-called two phase model in which the polymerization proceeds through three stages depending on the total number of phases present inthe polymerization reactor.[14−22] Generally speaking, the approaches described in literature differ mainly in the level of detail that is considered in the kinetic model and in the method used to account for diffusion limitations.

Kinetic Model. Most kinetic models describe the polymerization based on a reaction network taking into account a rather limited set of reactions. Talamini et al.,[17,18] Kiparissides et al.,[16] and De Roo et al.[19,20] use a kinetic model based on a reaction network including initiation, propagation, chain transfer to monomer, and termination by combination and disproportionation. The reaction network presented by Xie et al.[14,15] includes a more extended set of reactions, including backbiting and chlorine shift reactions. However, these authors solely investigated the effect of process conditions on the polymerization rate and did not focus on the formation of structural defects. Krallis et al.[21] introduce a model that is able to describe the suspension polymerization of vinyl chloride initiated by a combination of mono- and bifunctional initiators. This is done by applying a reaction network that is built up from an extended set of elementary reactions. The authors focus on the effect of using multifunctional initiators on the polymerization process. Wieme et al.[22] introduced a methodology to account for the formation of structural defects in the suspension polymerization of

*Corresponding author. E-mail: MarieFrancoise.Reyniers@UGent.be. Fax: 0032 (0)9 2644999.

Published on Web 10/02/2009

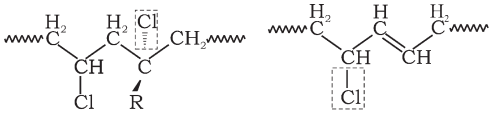

(a) tertiary chlorine (b) allylic chlorine

Figure 1. Tertiary and allylic chlorine in poly(vinyl chloride).

Table 1. Average Bond Dissociation Energies of the Bonds Present in the Reaction Mixture during the Free-Radical Suspension Polymerization of Vinyl Chloride[12,13]

bond	BDE (kJ mol^{-1})	bond	BDE (kJ mol^{-1})
C−C	350−380	C−Cl	330
C=C	611	C−Cl (allylic)	243
C−H	410	C−Cl (tertiary)	281
C−O	350	O−O	145

vinyl chloride. The applied methodology comprises a reaction network built up from structurally distinct radical and polymer species and an extended set of elementary reactions.

In the present contribution, based on the methodology developed by Wieme et al.,[22] the free radical polymerization of vinyl chloride is modeled at the elementary reaction level, explicitly focusing on the formation of structural defects. The set of elementary reactions that is accounted for is chosen carefully to capture the chemistry of interest. The latter involves not only the classical polymerization reactions, e.g., radical addition and recombination reactions, but also reactions specific to the formation of structural defects, e.g., intramolecular H-abstraction and 1,2 Cl-shift reactions. The presented kinetic model is applied to investigate the formation of defects as a function of polymerization time for a set of industrially representative polymerization conditions.

Diffusion Limitations. During the course of the polymerization process, the viscosity of the reaction medium increases significantly and reactions can become diffusion-controlled. It is therefore important to account for the effect of diffusion on kinetics when modeling the suspension polymerization process. The method used to model diffusion in the above-mentioned models varies strongly and influences to a large extent the conclusions that can be drawn from the results. Therefore, when evaluating different modeling efforts, it is important to consider to what level of detail transport limitations have been accounted for. In the model of Xie et al.[14,15] and of Talamini et al.[17,18] diffusion parameters are estimated from a set of experimental data to enable calculation of diffusional limitations on the polymerization reactions. In the model of Kiparissides et al.[16] and of Krallis et al.[21] diffusional limitations are accounted for by implementing a generalized free volume theory to calculate the diffusion coefficients and adjusting some of the diffusion parameters to experimental data. In the model of De Roo et al.[19,20] a general approach for the independent calculation of diffusion effects on polymerization reactions is applied. All the apparent rate coefficients are consistently calculated based on an intrinsic rate coefficient and a diffusion contribution. This diffusion contribution is modeled using the Smoluchowski theory. The diffusion coefficients in these diffusion contributions are calculated based on the physical properties of the components in the reaction mixture using the free volume theory, hence avoiding the need for adjustable diffusion-related parameters.

In this work, the method of De Roo et al.[19,20] to account for the effect of diffusion on reaction is used. Although it can be expected that there will always be some influence of the applied diffusion model on the intrinsic kinetics, a systematic and consistent approach to account for diffusion effects will increase the accuracy of the model.

Table 2. Overview of Structural Defects in PVC, Their Content in Commercial PVC Samples (Obtained from the Literature and Expressed as a Number of Defects per 1000 Monomer Units) and Their Relation to the Thermal Stability (TC = Tertiary Chlorine, AC = Allylic Chlorine)

branch type	content [no. per 1000 VC units][a]	thermal stability
chloromethyl	3.5−4.8	
1,2-dichloroethyl	0.4−0.5	
2,4-dichlorobutyl	1.5−1.8	TC
long chain branch	0.5−2.0	TC
unsaturations	0.3−0.9	AC

[a] Starnes et al.,[23,25,26] Hjertberg et al.,[3] Guyot,[6] Llauro-Darricades et al.,[27] and Purmova et al.[9]

This article is organized as follows: section 2 comprises a description of the kinetic model in which the construction of the reaction network is discussed. The selection of the species and the reactions to be considered in this reaction network is performed based on the polymerization chemistry and the chemistry involved in the formation of structural defects. The derivation of model equations, being mass balances and moment equations, starting from the developed reaction network is also discussed.

In sections 3 and 4 the presented model is validated by comparing simulated and experimental data for monomer conversion, averages of the molar mass distribution and for the structural defects content. To our knowledge, the developed model is the first that allows to predict both monomer conversion, averages of the molar mass distribution and the content of structural defects over the entire conversion range for a range of industrially relevant polymerization conditions.

2. Kinetic Model

In general, a kinetic model describing the free-radical polymerization of vinyl chloride includes chain initiation, propagation, chain transfer to monomer and bimolecular termination reactions. However, there is strong evidence that in the free radical polymerization of vinyl chloride reactions such as chain transfer to monomer and formation of short and long chain branches involve a sequence of elementary reaction steps.[15,23] The presence of defects in PVC validates the conclusion that several types of radicals are formed throughout the polymerization process, implying that other reactions than the ones mentioned above must also occur.[21,24]

2.1. Formation of Structural Defects. The most frequently occurring structural defects in PVC are branches and unsaturations. A distinction can be made between short ($\leq$4C atoms) and long ($>$4C atoms) chain branches on the one hand and unsaturations on the other hand. Table 2 gives an overview of the literature data that have been reported on the structural defects content in PVC. All structures mentioned in Table 2 are depicted in Figure 2. It should be noted that apart from the structures mentioned in Table 2, also other branch structures have been the subject of discussion, e.g., 2-chloroethyl branches,[25] pentyl branches,[23] 1,3-bis(2-chloroethyl) branches.[28] However, as the concentration of these defects is below the detection limit of experimental techniques used to determine the structural defects content, no conclusive experimental evidence for their presence is available. Moreover, as their concentration is so low, their negative impact on the thermal stability of PVC will be significantly smaller compared to that of the defects mentioned in Table 2. Therefore, the formation of these structures has not been accounted for in the construction of the reaction network.

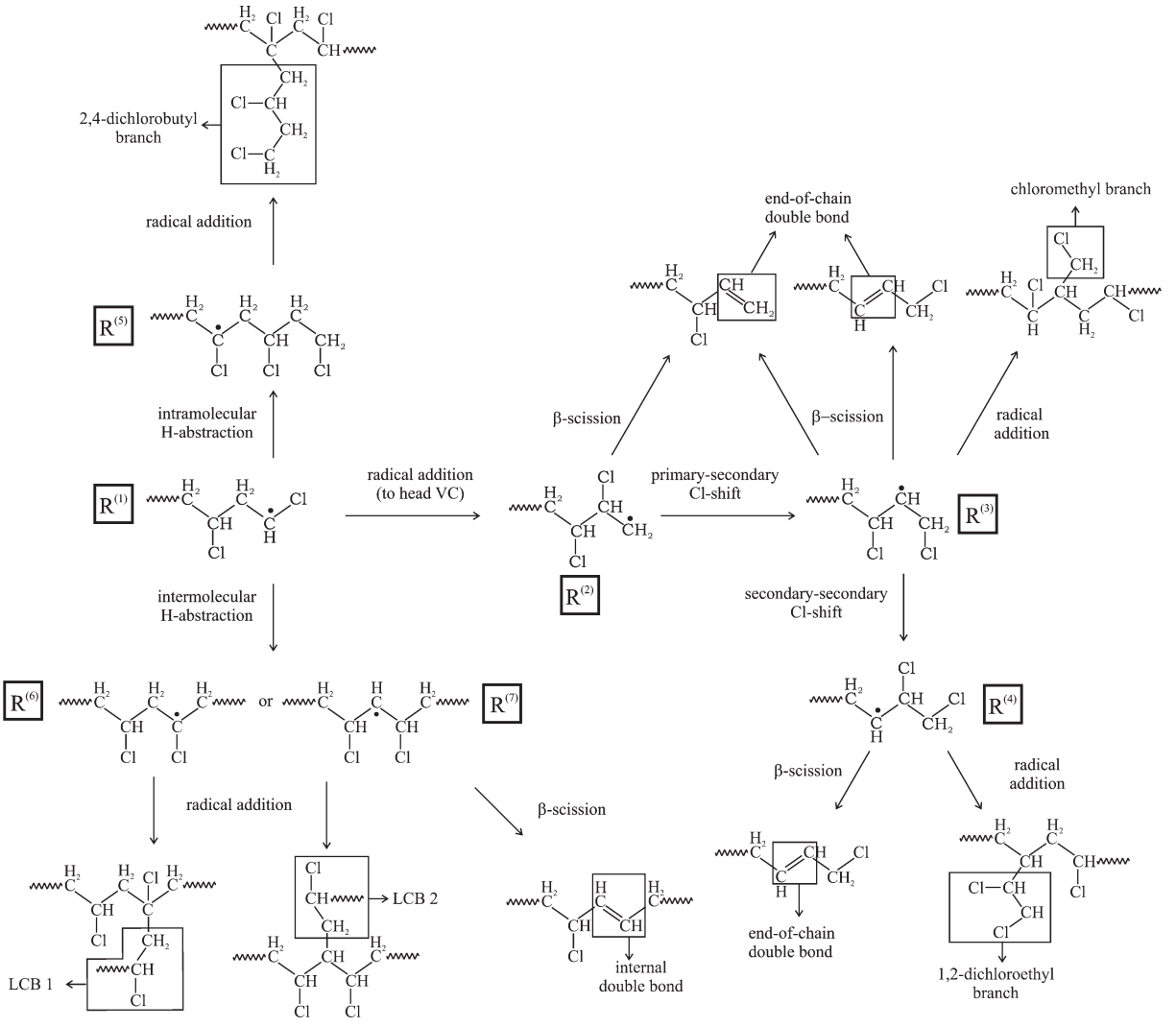

Figure 2. Reaction mechanism leading to the formation of the most important structural defects in vinyl chloride suspension polymerization.

From the structural defects depicted in Figure 2 it is clear that not all defects contain weakened carbon-chlorine bonds. Chloromethyl and 1,2-dichloroethyl branches do not imply the presence of tertiary chlorine and/or allylic chlorine. Hence, these structural defects have a lesser impact on the thermal stability. Their formation should however be considered when modeling the polymerization process as this is important to understand the polymerization kinetics.

In what follows the formation of the structural defects mentioned in Table 2 is discussed. On the basis of these mechanisms a set of reactions is selected that allows for the description of the formation of branches and unsaturations in the vinyl chloride suspension polymerization.

Chloromethyl Branches. Two mechanisms for the formation of chloromethyl branches have been proposed.[29] The first route, illustrated in Figure 2, originates from Rigo et al.[30] and postulates an addition of a radical of type $R^{(1)}$ to the head of a monomer unit, followed by a rearrangement of the resulting primary radical $R^{(2)}$ into a more stable secondary radical $R^{(3)}$ via a primary-secondary 1,2-chlorine shift. Subsequent addition of this radical $R^{(3)}$ to monomer generates a chloromethyl branch. The alternative mechanism, proposed by Starnes et al.[29] and Purmova et al.,[9] also involves radical $R^{(3)}$, but this time formed by a 1,2 H-shift of radical $R^{(1)}$. The latter seems unlikely owing to the stabilization of the radical site in radical $R^{(1)}$ by a chlorine atom. Moreover, no H-shifts have been reported in solution.[29]

From Figure 2 it can be seen that the formation of methyl branches involves the presence of different types of radicals in the reaction mixture, which are depicted as $R^{(s)}(s = 1, ..., 7)$. Therefore, when modeling the formation of structural defects in general and of chloromethyl branches in particular, it is necessary to account for the presence of these different radical types, as will be discussed in section 2.3.

1,2-Dichloroethyl Branch. Two types of ethyl branches are thought to occur in poly(vinyl chloride): the 2-chloroethyl and the 1,2-dichloroethyl branch.[23] The 2-chloroethyl branch is thought to be formed via a 1,3 H-shift of radical type $R^{(1)}$ and the subsequent addition of the formed radical to monomer. This mechanism implies that 2-chloroethyl branches contain tertiary chlorine. Starnes et al.[25] showed that the ethyl branches in commercial poly(vinyl chloride) do not contain tertiary chlorine, hence excluding the occurrence of 2-chloroethyl branches. In agreement with the findings of Starnes et al.,[25] the formation of 2-chloroethyl branches has not been accounted for in the construction of the polymerization reaction network.

The mechanism leading to the formation of the 1,2-dichloroethyl branch starts with an addition of a macroradical $R^{(1)}$ to the head of vinyl chloride (VC), followed by a primary-secondary 1,2 chlorine shift of radical $R^{(2)}$, which in its turn undergoes a secondary-secondary 1,2 chlorine shift.[25] Further addition of the formed radical $R^{(4)}$ to monomer results in the

formation of a 1,2-dichloroethyl branch, as is shown in Figure 2.

2,4-Dichlorobutyl Branch. Butyl branches in PVC are known to be formed via a unimolecular reaction.[23,31] The mechanism of the formation of the 2,4-dichlorobutyl branch starts with a 1,5 intramolecular hydrogen abstraction of radical $R^{(1)}$ involving a six-membered transition state and creating a radical $R^{(5)}$.[31,32] The latter reaction is also called a backbiting reaction. Further addition of the formed radical $R^{(5)}$ to monomer results in the formation of a 2,4-dichlorobutyl branch, as is shown in Figure 2. The experimental evidence in favor of this reaction mechanism consists of the finding that the butyl branching content increases significantly at high monomer conversions, which can be explained by the favoring of the unimolecular backbiting reaction over bimolecular reactions at these conditions.

As can be seen from Figure 2, the branching point bearing a 2,4-dichlorobutyl branch involves the presence of tertiary chlorine. Therefore, this type of branching has a negative impact on the thermal stability of poly(vinyl chloride).

Long Chain Branches. Long chain branches are formed when mid chain radicals ($R^{(6)}$ and $R^{(7)}$ in Figure 2), formed by an intermolecular hydrogen abstraction, add to monomer: viz. Figure 2.[3,23] Depending on where along the backbone of the polymer molecule a hydrogen is abstracted, a distinction can be made between long chain branches located at a branching point containing a tertiary chlorine (LCB1) or a tertiary hydrogen (LCB2). Only long chain branches involving tertiary chlorine (LCB1) are known to be detrimental toward the thermal stability of poly(vinyl chloride).

Since both radicals $R^{(6)}$ and $R^{(7)}$ result from H-abstraction reactions involving a polymer molecule, long chain branches can only be formed in the polymer-rich phase since polymer molecules that are formed in the monomer-rich phase are considered to immediately precipitate into the polymer-rich phase.

Unsaturations. A distinction can be made between internal and end-of-chain unsaturations, as is also shown in Figure 2. Unsaturated structures in poly(vinyl chloride) are known to result from chain transfer to monomer reactions and/or disproportionation reactions.[23,33] However, as reported by De Roo et al.,[20] termination in the free radical polymerization of vinyl chloride occurs predominantly by recombination. For this reason, the disproportionation reaction is not considered in the construction of the reaction network.

Chain transfer to monomer proceeds via several reaction mechanisms[24,33] and is in all cases the result of a sequence of elementary reaction steps.[8,33] The first set of reaction mechanisms labeled as chain transfer to monomer results in the formation of terminal double bonds and starts with the formation of radical type $R^{(2)}$ via the addition of a radical R^1 to the head of a monomer molecule. The formation of terminal double bonds then proceeds via the breaking of a carbon-chlorine bond in β position to the radical center. The breaking of such a C−Cl bond is only possible for radicals $R^{(2)}$, $R^{(3)}$, and $R^{(4)}$. The latter two radicals are formed by one or more successive 1,2 Cl-shifts starting from radical $R^{(2)}$, as can be seen from Figure 2.

The second reaction mechanism labeled as chain transfer to monomer results in the formation of internal double bonds and starts with the abstraction of a hydrogen atom at a CH_2 group along the backbone of the polymer chain. By breaking the carbon−chlorine bond in β position to the radical center in the hence formed radical $R^{(7)}$, an internal double bond is formed.

The breaking of the carbon−chlorine bond in the β position to the radical center is often considered as a bimolecular reaction step involving a monomer molecule, based on the argument that Cl radicals cannot become kinetically free.[23,33] This is however contradictory to the findings of De Roo et al.,[19] who showed that the presence of Cl radicals is necessary to fully explain the gel effect in the suspension polymerization of vinyl chloride. The latter is in line with Xie et al.[15] and Hjertberg and Sörvik,[4] who also consider the presence of chlorine radicals in the free radical polymerization of vinyl chloride. It should be noted that regardless of the considered reaction mechanism the outcome of the chain transfer to monomer process is identical because the most likely reaction possibility of Cl radicals is the addition to vinyl chloride. Only at high monomer conversions, when the monomer concentration decreases significantly, the probability that chlorine radicals will undergo reactions other than addition to a monomer unit increases. In this work, the unimolecular elimination of Cl by means of a β-scission reaction is considered for the construction of the reaction network.

Note that Purmova et al.[10] also attribute the formation of terminal double bonds to 1−6 intramolecular hydrogen abstraction reactions, resulting in a double bond between carbons 5 and 6 in the polymer chain. However, the ratio of the ab initio calculated rate coefficients of the 1−5 to the 1−6 intramolecular hydrogen abstraction rate coefficient is close to 1500 at 330 K. Hence, it is justified to conclude that the main route toward terminal double bonds proceeds via 1−5 intramolecular hydrogen abstraction reactions and to neglect the 1−6 intramoleculare hydrogen abstraction reaction in the construction of the reaction network. From Figure 2 it can also be seen that only radicals $R^{(1)}$ are considered to undergo 1−5 hydrogen abstraction reactions. Purmova et al. also suggest 1−5 backbiting reactions of radicals $R^{(3)}$ as a possible route toward the formation of terminal double bonds. The rate coefficient of this reaction step is however calculated to be 20 times lower than the 1−5 backbiting reaction of radical $R^{(1)}$. On the basis of this argumentation, this reaction is omitted from the reaction network.

2.2. Elementary Reaction Families. On the basis of the mechanisms of formation of the most frequently occurring structural defects, it can be concluded that describing structural properties of the polymer product such as branching and unsaturation content is not possible when accounting for a limited set of reactions only. The formation of the defects implies that reactions other than chain initiation, propagation, chain transfer to monomer and bimolecular termination occur, as is mentioned in section 2.1. In the present study, the free radical suspension polymerization of vinyl chloride is modeled at the elementary reaction level, systematically taking into account diffusional limitations. The radical reactions involved in the polymerization process are grouped according to reaction families, consisting of forward and reverse reaction steps: bond dissociation and radical recombination, addition to a carbon−carbon double bond and β-scission, hydrogen abstraction, and 1,2-chlorine shift. An overview of all considered reactions is given in Table 3. All reactions, apart from the intermolecular hydrogen abstraction reactions were considered to occur in both the monomer-rich and the polymer-rich phase. Intermolecular hydrogen abstraction reactions involve the presence of polymer molecules. As polymer molecules that are formed in the monomer-rich phase are considered to immediately precipitate into the polymer-rich phase,[16,20] this reaction can only take place in the polymer-rich phase. By applying the above-mentioned set of elementary reactions to the species in the reaction mixture, the reaction network is generated.

Bond Dissociation. Table 1 shows the bond dissociation energies of all bonds present in the reaction mixture.

Table 3. Overview of the Reactions Considered in the VC Suspension Polymerization

reaction	considered	motivation	k
bond dissociation of carbon−carbon single bond	no	BDE[a]	
bond dissociation of carbon−carbon double bond	no	BDE[a]	
bond dissocisation of carbon−hydrogen bond	no	BDE[a]	
bond dissociation of carbon-chlorine bond	no	BDE[a]	
bond dissociation of carbon−oxygen bond	no	BDE[a]	
bond dissociation of oxygen−oxygen bond	yes		k_{bd}
radical recombination (C−C)	yes		k_{rc}^{ij}
radical recombination (C−Cl)	yes		k_{rCl}
radical recombination (C−O)	no		
radical recombination (Cl−Cl)	no	exp[b]	
radical recombination (Cl−O)	no	exp[b]	
radical recombination (O−O)	yes/no	lit[c]	
radical addition of C-centered radical to nonsubstituted C of VC (tail)	yes		k_{at}^{s}
radical addition of C-centered radical to substituted C of VC (head)	yes		k_{ah}^{s}
radical addition of C-centered radical to terminal double bond	yes		$k_{aedb,k}$
radical addition of C-centered radical to internal double bond	yes		$k_{aidb,k}$
radical addition of Cl-centered radical to nonsubstituted C of VC (tail)	yes		k_{aCl}
radical addition of Cl-centered radical to substituted C of VC (head)	no	exp[b]	
radical addition of Cl-centered radical to terminal double bond	yes		$k_{aedbCl,k}$
radical additionof Cl-centered radical to internal double bond	yes		$k_{aidbCl,k}$
radical addition of O-centered radical to nonsubstituted C of VC (tail)	yes		k_{a0}
radical addition of O-centered radical substituted C of VC (head)	no	exp[b]	
β-scission of C−Cl bond	yes		k_{β}
β-scission of C−C bond	no	BDE[a]	
β-scission of C−H bond	no	BDE[a]	
primary-secondary 1,2 Cl-shift	yes		k_{Clps}
secondary-secondary 1,2 Cl-shift	yes		k_{Clss}
intermolecular H-abstraction by C-centered radical at CH_2 group	yes		k_{Hc}
intermolecular H-abstraction by C-centered radical at CHCl group	yes		k_{Hc*}
intermolecular H-abstraction by Cl-centered radical at CH_2 group	yes		k_{HCl}
intermolecular H-abstraction by Cl-centered radical at CHCl group	yes		k_{HCl*}
intermolecular H-abstraction by O-centered radical at CH_2 group	no	exp[b]	
intermolecular H-abstraction by O-centered radical at CHCl group	no	exp[b]	
intramolecular H-abstraction (1,5 backbiting)	yes		k_{H15}
intramolecular H-abstraction (1,4-backbiting)	no	exp[b]	

[a] The bond dissocation energy of the bond that needs to be broken is too large. [b] Structures resulting from these reactions have not been detected experimentally. [c] The bond dissociation rate coefficients of oxygen−oxygen bonds that have been experimentally obtained include the reverse reaction of the dissociation as well. Therefore, the oxygen−oxygen recombination reaction is implicitly taken into account; however, no separate rate coefficient is used for this reaction.

Given the large difference in bond dissociation energy between the oxygen−oxygen bond and the weakest bond present in PVC (the difference is approximately100 kJ mol^{-1}), it is assumed that homolytic scission of bonds other than the oxygen−oxygen bond does not occur.

Radical Recombination. The recombining radicals can be either carbon-centered, chlorine-centered or oxygen-centered radicals, viz. Figures S.1(b), S.1(c), and S.1(d) (see Supporting Information). Since recombination products of two chlorine-centered radicals and of a chlorine-centered and an oxygen-centered radical have not been detected experimentally, these recombination reactions are not taken into account in the reaction network. The recombination of oxygen-centered radicals originating from the initiator molecules and carbon-centered radicals is implicitly taken into account by introducing an initiator efficiency.

Radical addition. The radical can add to the double bond at the nonsubstituted carbon atom (tail addition), or at the substituted carbon atom (head addition), viz. Figures S.1(e), S.1(f), S.1(i), and S.1(l) (see Supporting Information). Radicals can also add to internal and end-of chain double bonds, as is shown in Figures S.1(g)−S.1(h) and S.1(j)−S.1(k) (see Supporting Information).

β-Scission. β-Scission of carbon−carbon and carbon−hydrogen bonds are not considered because of the higher strength of these bonds, cf. Table 1. Moreover, no experimental evidence for the occurrence of these reactions within the range of industrially applied polymerization conditions has been mentioned in literature.

1,2-Chlorine Shift. Depending on the position of the migrating chlorine radical a distinction can be made between a primary-secondary 1,2 Cl-shift, in which a primary carbon-centered radical is transformed into a secondary carbon-centered radical, cf. Figure S.1(n), and a secondary-secondary 1,2 Cl-shift, in which a secondary carbon-centered radical remains a secondary carbon-centered radical, cfr. Figure S.1(o).

Hydrogen Abstraction. Both carbon-centered and chlorine-centered radicals are known to abstract hydrogen atoms, cfr. Figures S.1(p), S.1(q), S.1(r), and S.1(s). The intramolecular hydrogen abstraction is a 1,5 backbiting reaction, implying a six-membered transition state, cfr. Figure S.1(t). The analogous reaction with a more strained five-membered transition state is not considered, since the resulting branch structure is not detected in PVC. Note that Purmova et al.[10] also consider intramolecular 1,2. 1,3. 1,4, and 1,6 hydrogen abstraction reactions. The rate coefficients obtained for these reactions via ab initio calculations are however significantly lower than the rate coefficient obtained for the 1,5 intramolecular hydrogen abstraction reaction, hence justifying the removal of these reaction steps from the reaction network.

2.3. Network Generation. Generating the reaction network is done by applying the above-mentioned set of elementary reaction families to all species present in the reaction mixture. Initially, only initiator and monomer molecules are present in the reaction mixture, as is schematically shown in Figure 3.

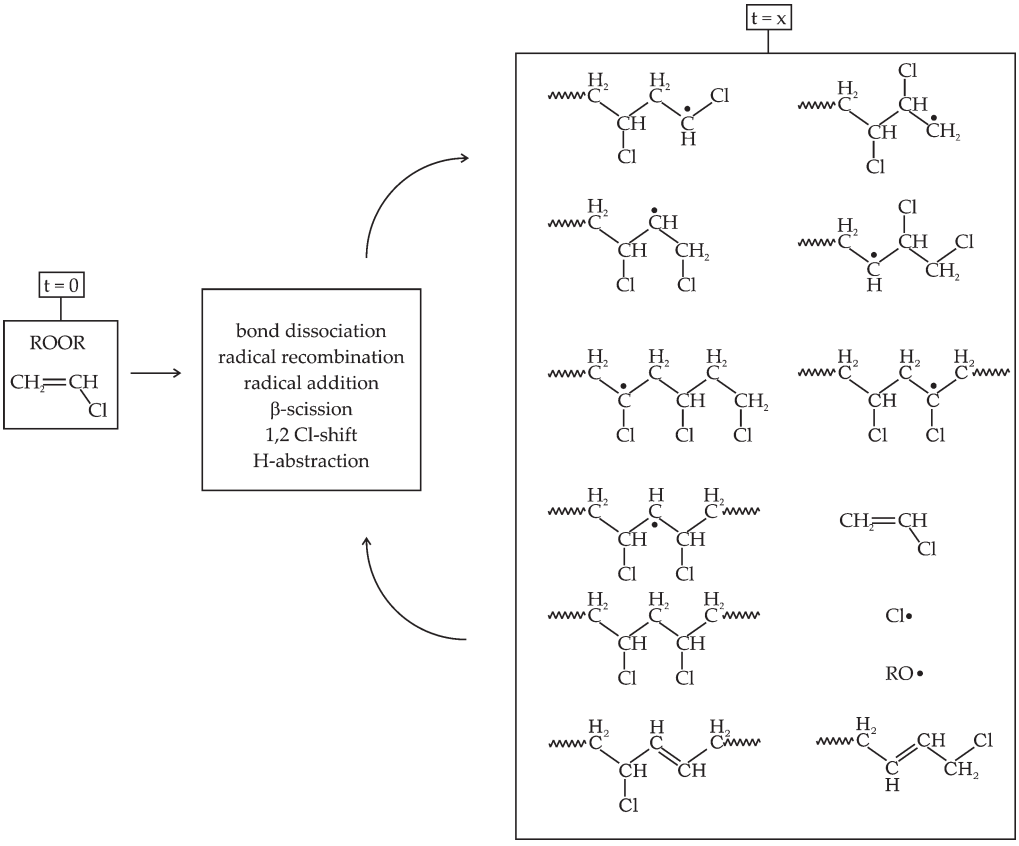

Figure 3. Schematic representation of the reaction network generation.

At a given time during the polymerization process a wide range of macroradicals and polymer molecules are present in the reaction mixture. Next to the chain length, macroradicals also differ by the structure of their radical center. All macroradicals are carbon-centered radicals, but the molecular structure in the proximity of the radical can vary, implying different reaction possibilities.

All macroradical structures are therefore classified into seven groups according to the structure of their radical center. Figure 2 illustrates the formation of the various radical types starting from the radical resulting from the addition to the tail of VC.

It should be noted that not all radical types can undergo all reactions mentioned above. Table S.1 in the Supporting Information gives an overview of which reactions are considered for each radical type. On the basis of these considerations, the mass balances for all seven radical types and polymer molecules are constructed.

Within the group of polymer molecules a distinction is made between saturated and unsaturated molecules. This distinction is necessary because unsaturated polymer molecules can undergo addition reactions with all radical structures in the reaction mixture whereas saturated polymer molecules cannot. Therefore, it is necessary to account for both types of polymer molecules separately. Within the group of unsaturated polymer molecules a further distinction is made between polymer molecules containing an internal or a terminal double bond.

2.4. Model Equations. In order to be able to calculate the monomer conversion, the averages of the MMD and the structural defects content as a function of polymerization time and polymerization conditions, the variation of the concentration of all radicals and polymer molecules needs to be known. To that end, the mass balances of all species present in the reaction mixture are constructed, based on the reaction network as presented in section 2.3.

The method of moments is used to calculate the moments of the molar mass distribution of the radicals and the polymer molecules, hence reducing the large number of mass balances to be solved.

2.4.1. Mass Balances. As is also described in section 2.3, macroradicals differ not only by chain length but also by the structure of their radical center, the latter determining the reactions that need to be taken into account for each radical type. The combination of these two aspects results in a very large number of distinct species, hence exceeding the computational feasibility of tracking all individual species.

As was discussed in section 2.3, the macroradicals can be grouped into seven different groups. For the initiator, the monomer, the chlorine radicals, the macroradicals of type s and with chain length i, $R_{i,k}^{(s)}$ (i = 1, ..., ∞, s = 1, ..., 7) and for the polymer molecules with chain length i ($P_{i,k}^{\mathrm{sat}}$, $P_{i,k}^{=\mathrm{end}}$ and $P_{i,k}^{=,\mathrm{int}}$; i = 1, ..., ∞) the mass balances are given Table S.2 in the Supporting Information.

For the initiator derived radicals, $R_{0,k}$, the quasi steady-state approximation is applied:

$$\frac{1}{V_k}\frac{\mathrm{d}V_k R_{0,k}}{\mathrm{d}t} = 2f_k k_{bd,k} I_k - k_{aO,k} R_{0,k} M_k \approx 0 \qquad (1)$$

Resulting in

$$R_{0,k} = \frac{2f_k k_{bd,k} I_k}{k_{aO,k} M_k} \qquad (2)$$

As the polymerization takes place in the monomer-rich and in the polymer-rich phase, but not in the gas phase nor

in the water phase, the monomer conversion is calculated from:

$$\frac{dX}{dt} = -\frac{1}{M_0}\frac{d\left(\sum_{k=1}^{2} V_k M_k\right)}{dt} \quad (3)$$

Note that in the mass balances in Table S.2 in the Supporting Information, it is assumed that no transfer of radicals between the monomer-rich phase and the polymer-rich phase occurs. In contrast to, e.g., emulsion polymerization processes, it is well-known that a transfer of radicals between the reactive phases influences the suspension polymerization processes of vinyl chloride to a rather small extent.[16,34] Accounting for a transfer of radicals between both phases is shown to be important at low polymerization temperatures only (i.e., 308 K).[34] At higher polymerization temperatures the effect of accounting for radical transfer is much less pronounced as the exchange surface area between the monomer-rich and the polymer-rich phase is low at higher temperatures.[34] In this work the investigated temperatures exceed the temperatures at which a significant effect of a transfer of radicals on the model calculations can be expected. Therefore, no transfer of radicals is accounted for. Moreover, the polymer molecules formed in the monomer-rich phase immediately precipitate in the polymer-rich phase as they are insoluble in the monomer.

For the calculation of the partitioning of the monomer and the initiator over the phases in the reactor, the conversion at which the transition of the second to the third stage occurs and the mass and volume calculations of the different phases reference is made to De Roo et al.[20]

2.4.2. Moment Equations. The method of moments is used to calculate the average properties of the molar mass distribution (M_n, M_m). This significantly reduces the number of balances to be solved. M_n and M_m are a function of the averages of the molar mass distribution of the polymer in both phases ($M_{n,k}$ and $M_{m,k}$) and the fraction of monomer consumed in each phase by polymerization ($\omega_{pol,k}$):

$$M_n = \frac{1}{\omega_{pol,1}/M_{n,1} + \omega_{pol,2}/M_{n,2}} \quad (4)$$

$$M_m = \omega_{pol,1} M_{m,1} + \omega_{pol,2} M_{m,2} \quad (5)$$

The averages of the molar mass distribution of the polymer molecules in each phase ($M_{n,k}$, $M_{m,k}$ with $k = 1, 2$) are calculated from the ratio of the moments of the polymer distribution in each phase.

$$M_{n,k} = \frac{\mu_{1,k}}{\mu_{0,k}} \quad (6)$$

$$M_{m,k} = \frac{\mu_{2,k}}{\mu_{1,k}} \quad (7)$$

The ath order moment of the distribution of all polymer molecules is obtained from the moments of the saturated polymer molecules ($\mu_{a,k}^{sat}$) and the unsaturated polymer molecules ($\mu_{a,k}^{=end}$, $\mu_{a,k}^{=int}$):

$$\mu_{a,k} = \mu_{a,k}^{sat} + \mu_{a,k}^{=,end} + \mu_{a,k}^{=,int} \quad (8)$$

The ath order moment of the distribution of the saturated ($\mu_{a,k}^{sat}$) and unsaturated polymer molecules ($\mu_{a,k}^{=end}$ and $\mu_{a,k}^{=int}$) is defined as ($a = 0, ..., 2$):

$$\mu_{a,k}^{sat} = \sum_{i=1}^{\infty} i^a P_{i,k}^{sat} \quad (9)$$

$$\mu_{a,k}^{=,end} = \sum_{i=1}^{\infty} i^a P_{i,k}^{=,end} \quad (10)$$

$$\mu_{a,k}^{=,int} = \sum_{i=1}^{\infty} i^a P_{i,k}^{=,int} \quad (11)$$

Analogously, the ath order moment of the distribution of macroradicals of class$s$, $\lambda_{a,k}^{(s)}$, is given by:

$$\lambda_{a,k}^{(s)} = \sum_{i=1}^{\infty} i^a R_{i,k}^{(s)} \quad (12)$$

The moments of the macroradical distribution of type s in phase k, $\lambda_{a,k}^{(s)}$, are required to calculate the moments of the polymer distribution in phase k, $\mu_{a,k}$

The equations for the moments of the macroradical distributions and the polymer distribution in the monomer-rich phase and in the polymer-rich phase are presented in Tables S.3−S.5 in the Supporting Information. These equations need to be integrated together with the mass balances for the monomer (eq S.1), the chlorine radicals (eq S.2) and the initiator (eq S.3).

When deriving the moment equations, the terms related to the recombination of two macroradicals and the intermolecular H-abstraction reaction involving a macroradical require the knowledge of the concentration of each radical belonging to a certain radical type s with a given chain length$i$, $R_{i,k}^{(s)}$. These concentrations are obtained by solving the algebraic eqs S.4−S.15 resulting from the application of the quasi steady-state approximation to the macroradicals $R_{i,k}^{s}$ using a coarse-graining technique.[20,35,36]

The fraction of monomer consumed in each phase by polymerization, $\omega_{pol,k}$, is calculated from:

$$\omega_{pol,1} = \frac{\int_0^t R_{pol,1}^V V_1 m m_m \, dt'}{\int_0^t (R_{pol,1}^V V_1 + R_{pol,2}^V V_2) m m_m \, dt'} \quad (13)$$

$$\omega_{pol,2} = 1 - \omega_{pol,1} \quad (14)$$

in which $R_{pol,k}^V$is the polymerization rate in phase k (k = 1,2). The latter is calculated from:

$$R_{pol,k}^V = 2 f_k k_{bd,k} I_k + \sum_{s=1}^{7} (k_{at,k}^s + k_{ah,k}^s) M_k R_{tot,k}^{(s)} + k_{aCl,k} M_k Cl_k \quad (15)$$

The above-mentioned equations are solved numerically with an ordinary differential equation (ODE) solver.[37] The LSODA (Livermore solver for ordinary differential equations, with automatic switching for stiff and nonstiff problems) subroutine uses the Adams method for nonstiff ODEs and a BDF (backward differentiation formula) method for stiff ODEs.

Table 4. Arrhenius Parameters of the Intrinsic Rate Coefficients of the Reactions Considered during the Suspension Polymerization of Vinyl Chloride

no.	reaction			A [m^3 mol^{-1} s^{-1} or s^{-1}]	E_a [$kJmol^{-1}$]	ref
1	bond dissociation	(O−O,dimyristyl peroxydicarbonate)	$k_{bd,chem}$	2.82×10^{15}	124.1	20
2	bond dissociation	(O−O, dicetyl peroxydicarbonate)	$k_{bd,chem}$	3.02×10^{15}	124.3	20
3	radical recombination	(C−C)	$k_{rc,chem}$	7.1×10^{4}	0.0	20
4		(C−Cl)	$k_{rCl,chem}$	7.9×10^{4}	0.0	20
5	radical addition to C=C	(C, to tail of VC)	$k^s_{at,chem}$	9.3×10^{3}	24.9	20
6		(C, to head of VC)	$k^s_{ah,chem}$	9.3×10^{3}	30.9	20
7		(C, to terminal DB)	$k_{aedb,chem}$	9.3×10^{2}	24.9	20
8		(C, to internal DB)	$k_{aidb,chem}$	9.3×10^{2}	24.9	20
9		(Cl, to tail of VC)	$k_{aCl,chem}$	2.3×10^{4}	28.4	20
10		(Cl, to terminal DB)	$k_{aedbCl,chem}$	2.3×10^{3}	28.4	20
11		(Cl, to internal DB)	$k_{aidbCl,chem}$	2.3×10^{3}	28.4	20
12	β-scission		$k_{\beta,chem}$	5.5×10^{6}	41.6	10
13	1,2 Cl-shift	primary−secondary	$k_{Clps,chem}$	1.6×10^{13}	43.0	10,24
14		secondary−secondary	$k_{Clss,chem}$	1.4×10^{13}	48.1	10,24
15	H-abstraction	intermolecular by C from CHCl	$k_{Hc,chem}$	3.1×10^{3}	50.1	16,24
16		intermolecular by C from CH_2	$k_{Hc*,chem}$	1.44×10^{3}	41.8	16,24
17		intermolecular by Cl from CHCl	$k_{HCl,chem}$	3.1×10^{3}	50.1	16,24
18		intermolecular by Cl from CH_2	$k_{HCl*,chem}$	1.44×10^{3}	41.8	16,24
19		intramolecular	$k_{H15,chem}$	3.6×10^{11}	64.8	10,24

2.4.3. Structural Defects Content Calculation. As is extensively discussed in section 2.1 and as can be seen from Figure 2, the formation of structural defects in the polymer product can be directly linked to the presence of the distinct radical types in the reaction mixture. The presence of chloromethyl, 1,2-dichloroethyl, 2,4-dichlorobutyl and long chain branches can be linked to the presence of radical types $R^{(3)}$, $R^{(4)}$, $R^{(5)}$, $R^{(6)}$, and $R^{(7)}$ respectively. To calculate the branching content rate of formation of the different branch types is considered to be equal to the rate of addition reactions involving radical types $R^{(3)}$, $R^{(4)}$, $R^{(5)}$, $R^{(6)}$, and $R^{(7)}$. The rate of formation of unsaturations is obtained from the rate of the β-scission reactions of radicals $R^{(2)}$, $R^{(3)}$, $R^{(4)}$, and $R^{(7)}$.

For each of the structural defects mentioned in Figure 2, the content is obtained by calculating the ratio of the cumulative rate of formation of the structural defect and the cumulative rate of polymerization:

$$\rho_x = \frac{\int_0^t (R_{x,1} V_1 + R_{x,2} V_2)\, dt}{\int_0^t (R^V_{pol,1} V_1 + R^V_{pol,2} V_2)\, dt} \tag{16}$$

in which $x = MB, EB, BB, LCB, EDB$. For a more detailed discussion on the calculation of the structural defects reference is made to section S.1 in the Supporting Information.

2.4.4. Combination of Reaction and Diffusion. In suspension polymerization of vinyl chloride, it is generally assumed that bimolecular reactions in the polymer-rich phase ($k = 2$) can become diffusion-controlled, while monomolecular reactions in the polymer-rich phase and all reactions in the monomer-rich phase ($k = 1$) are reaction-controlled.[14−16,18,20] Therefore, the observed rate coefficients (also called apparent rate coefficients) of the monomolecular reactions in the polymer-rich phase and all the reactions in the monomer-rich phase are considered to be related to the chemical reaction only and are equal to the intrinsic rate coefficients. The observed rate coefficients of bimolecular reactions in the polymer-rich phase are regarded as the sum of a reaction-related term and a diffusion-related term and are calculated as follows:[20,38]

$$\frac{1}{k_{app}} = \frac{1}{k_{chem}} + \frac{1}{k_{diff}} \tag{17}$$

The diffusional contribution, k_{diff}, is consistently modeled using the Smoluchowski expression for all diffusion-controlled reactions.[39] The diffusion coefficients in the Smoluchowski expression for k_{diff} are calculated based on the free volume theory. For a more detailed discussion on the calculation of the diffusion coefficients, reference is made to De Roo et al.[19,20]

The expression for the apparent initiator efficiency f_2 is chosen analogous to eq 17:

$$\frac{1}{f_2} = \frac{1}{f_{chem}} + \frac{1}{k_{f,diff}} \tag{18}$$

in which the intrinsic initiator efficiency f_{chem} is defined as the initiator efficiency in the absence of diffusional limitations. The value for f_{chem} is constant and is fixed for all calculations. The initiator efficiency in the monomer-rich phase f_1 is equal to f_{chem}. For the calculation of the diffusion contribution to the apparent initiator efficiency f_2, $k_{f,diff}$, reference is made to De Roo et al.[19,20]

Intrinsic Rate Coefficients. The Arrhenius parameters of the intrinsic rate coefficients k_{chem} of all considered elementary reaction families are mentioned in Table 4. All intrinsic rate coefficients are considered to be chain length independent. The reverse reactions of the reaction families shown in Figure S.1 have not been considered. Doing so would, among other things, allow to simulate the degradation of the polymer product.[40] However, under the investigated conditions it is wellestablished that no degradation reactions occur.

The values of the Arrhenius parameters for the bond dissociation reaction involving the initiator were obtained from the manufacturer (Akzo Nobel). The rate coefficients of the recombination reactions are taken from De Roo et al.[20]

The pre-exponential factor of all addition reactions to monomer involving C-centered radicals are taken equal to the value obtained by De Roo et al.[20] for the propagation reaction. For the activation energy of the addition of a C-centered radical to the head of a vinyl chloride molecule a value that is 6.0 kJ mol^{-1} higher as compared to the addition to the tail of vinyl chloride, has been reported by Endo.[12]

The Arrhenius parameters corresponding to the addition reaction of Cl-centered radicals to monomer are taken equal to the values obtained by De Roo et al.[20] for the Cl-initiation step, involving the addition of a Cl radical to a monomer molecule.

Mainly because of entropic factors, the rate coefficient for the addition to chloroallylic end groups and internal double bonds is approximately 1 order of magnitude less as compared

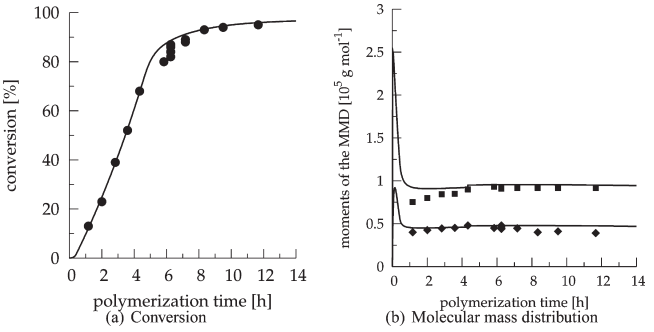

Figure 4. Comparison of experimental and simulated conversion and averages of the MMD. Polymerization conditions: $T = 330.65K$, concentration of the initiator 0.00069 wt %. (a) Monomer conversion as a function of polymerization time (●, experimental data obtained from Pauwels;[41] solid line, simulated data). (b) Averages of the molar mass distribution (♦) M_n and (■) M_m: experimental data obtained from Pauwels;[41] solid line, simulated data). Solid lines are calculated using equations in Tables S.2−S.5 with the set of intrinsic Arrhenius parameter values given in Table 4 and $f_{chem} = 1.0$.

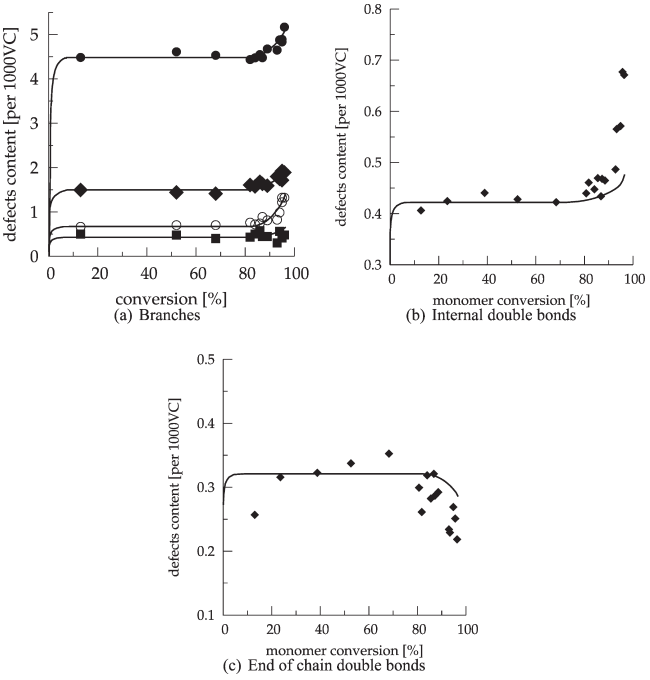

Figure 5. Comparison of experimental and simulated structural defects content. Polymerization conditions: $T = 330.65$ K, concentration of the initiator 0.00069 wt %. (a) Branch structures content as a function of monomer conversion (symbols are experimental data obtained from Purmova et al.:[9] (●) chloromethyl branches; (♦) 2,4-dichlorobutyl branches; (○) long chain branches; (■) 1,2-dichloroethyl branches; solid lines, simulated data). (b) Internal double bonds content as a function of polymerization time (symbols are experimental data obtained from Purmova et al.;[9] solid lines are simulated data). (c) End of chain unsaturations as a function of monomer conversion (symbols are experimental data obtained from Purmova et al.;[9] solid lines are simulated data). Solid lines are calculated using equations in Tables S.2−S.5 combined with eq 16. Intrinsic Arrhenius parameter values taken from Table 4 and $f_{chem} = 1.0$.

to that for the addition to vinyl chloride.[9] In agreement with these findings, the pre-exponential factor of these reaction steps is 1 order of magnitude less than the value for the addition reactions involving vinyl chloride.

For the β-scission involving a C−Cl bond Arrhenius parameters were chosen in accordance with the value reported by Purmova et al.[10] for the β-scission reaction involving a C−Cl bond.

For reactions 13−19 in Table 4, rate coefficients have been obtained based on ab initio calculations reported by Purmova et al.[10] and Van Cauter et al.[24] The ab initio calculated values were taken as initial guesses and adjusted to obtain a good fit to the experimental data reported by Purmova et al.[9] The pre-exponential factors of the hydrogen abstraction reactions are taken from Kiparissides et al.[16]

3. Simulation Results

In the following section, the presented kinetic model is validated by comparing simulated and experimental data for both monomer conversion, averages of the molar mass distribution and structural defects content. The experimental data were obtained from Purmova et al.[9] The experimental data presented in these studies are, to the best of our knowledge, the only available sets of data that allow to assess the formation of structural defects as a function of monomer conversion. As will be discussed further on, the variation of the reaction rates as a function of monomer conversion allows to fully explain the variation of the structural defects content as a function of polymerization conditions and polymerization time. All model calculations presented in this section account explicitly for temperature variations by implementing the experimentally measured temperature profiles, hence justifying the absence of energy balances in the model equations.

3.1. Monomer Conversion and Averages of the Molar Mass Distribution. In a recent publication, Purmova et al.[9] present a study on the influence of monomer conversion on the formation of structural defects. These authors reported ^{1}H and ^{13}C NMR analysis of a number of samples were taken over a large conversion range (13−95%). The samples were obtained by suspension polymerization in a 1 L reactor, filled with 350 mL of water. VC (175 g) and the initiator (dimyristyl peroxide) were added, and the temperature was increased to the polymerization temperature (330.5 K). Once the desired conversion was reached, a termination reagent was added and the reactor was cooled to 294 K. After removing the residual VC, the product mixture was filtered and the monomer conversion was measured by gravimetry.

Using our kinetic model we have simulated the experimental results reported by Purmova et al.[9] Figure 4 shows the comparison between simulated and experimentally obtained profiles for the monomer conversion (Figure 4a) and averages M_n and M_m of the molar mass distribution (Figure 1). It can be seen that our kinetic model can adequately simulate both the monomer conversion and the averages of the molar mass distribution as a function of polymerization time.

3.2. Structural Defects Content. Because of the importance of the structural defects for the physical properties of the final polymer product, a considerable number of studies on their formation have been performed in the past.[3,4,9,23,25−27,29−33,42,43] The main goal of these investigations was to determine how and to what extent structural defects in PVC are formed.

Most characterization procedures start with the reductive dehalogenation of PVC using $LiAlH_4$or Bu_3SnH. According to this technique, the chlorine atoms along the polymer chain are replaced by hydrogen atoms, hence converting PVC into a hydrocarbon. This hydrocarbon is then analyzed using spectroscopic techniques in order to deduce the structure of the starting polymer from that of the reduced product. The reduced polymer has been characterized structurally with a variety of analytical techniques, including ^{13}C and ^{1}H NMR spectroscopy, IR spectroscopy, pyrolysis−gas chromatography, and γ-radiolysis chromatography. However, it is commonly accepted that ^{1}H and ^{13}C NMR are the methods

of choice for total structure determinations, since these techniques provide the most information with minimal ambiguity.[23]

In the present contribution, the data presented by Purmova et al.[9] and Llauro-Darricades et al.[27] are used as a test case for our kinetic model. Both authors carried out a number of experiments to investigate the influence of monomer conversion on the content of structural defects formed in the suspension polymerization of vinyl chloride.

Structural Defects Content. Figure 5 shows a comparison between simulated and the by Purmova et al. experimentally obtained profiles for the structural defects content as a function of monomer conversion. Figure 5a shows the variation of the branching content as a function of monomer conversion, while parts b and c of Figure 5 show the unsaturation content as a function of monomer conversion. As can be seen, the content of branches is demonstrated to have the following order throughout the polymerization process: chloromethyl branches > 2,4-dichlorobutyl branches >long chain branches >1,2-dichloroethyl branches. It can also be seen that the content of all types of defect structures initially increases and subsequently remains rather constant for a large conversion range. From parts a and b of Figurs 5 it can be seen that, from a certain conversion on, the content of branches and internal double bonds increases again for increasing monomer conversions. From Figure 5c, however, a drop in the content of end-of-chain unsaturations is noticed at higher conversions.

The initial increase of the structural defects content profile can be explained by the higher activation energies of the reactions resulting in the formation of radicals leading to defects as compared to the activation energies of addition reactions, as can be seen from Table 4. Therefore, at lower temperatures, i.e., during the heating of the reactor, the formation of defects is hampered more than the consumption of monomer by addition reactions, explaining why the structural defects contentincreases at the start of the polymerization process.

Since the composition of both the monomer-rich and the polymer-rich phase remains constant throughout the second stage of the polymerization, the structural defects content remains constant until the start of the third stage of the polymerization. Once the monomer-rich phase disappears, i.e., at the start of the third stage of the polymerization, the monomer concentration in the polymer-rich phase drops and the viscosity of the polymer-rich phase increases, hence implying the presence of diffusional limitations. Therefore, two effects are responsible for the increase of the structural defects content as a function of monomer conversion during the third stage of the polymerization.

First, due to the drop in the monomer concentration, the unimolecular reactions will gain importance. Since most reactions responsible for the formation of radicals that lead to the formation of structural defects are unimolecular, the formation of structural defects gains in importance at these higher conversions. Internal double bonds originate from either inter- or intramolecular abstraction of hydrogen from the $-CH_2-$ group of the polymer chain, followed by β-scission of the resulting radical (see also Figure 2). Long chain branches and butyl branches originate from inter- or intramolecular hydrogen abstraction reactions, followed by addition to VC (see also Figure 2). The increase in the number of these defects at higher conversions can be understood in terms of the reduction of the monomer concentration in the polymer-rich phase. The methyl and ethyl branches are formed via the radical that results from an addition to the head of a monomer. If this radical undergoes a primary−secondary 1,2 Cl-shift and subsequently adds to monomer, a methyl branch is formed. In the case of a primary−secondary 1,2 Cl-shift followed by a secondary−secondary 1,2 Cl-shift, an ethyl branch is formed. Although the probability of an addition to the head of VC might be expected to remain relatively constant throughout the polymerization process, the probability that the subsequent radical undergoes a 1,2 Cl-shift increases as conversion increases and monomer concentration decreases, explaining the increase in the number of ethyl and methyl branches at high conversions.

Also, due to the increasing viscosity of the reaction mixture, diffusional limitations will become important at higher conversions in the polymer-rich phase. Again, since the unimolecular reactions are not hampered by diffusion limitations, their relativeimportance increases further with increasing monomer conversions. Because the unimolecular reactions are responsible for the formation of radicals that eventually lead to structural defects, the number of defects formed throughout the third stage of the polymerization increases significantly.

The increase of the branching content is in agreement with Purmova et al.[9] It should however be noted that, as is discussed in section 2.1, the presented kinetic model does not account for the formation of chloromethyl branches based on inter- or intramolecular hydrogen shift reactions, as is suggested by Purmova et al. Nevertheless, model calculations predict an increase of the chloromethyl branch content.

The above argumentation is illustrated in Figure 6 where the net rate of formation of chloromethyl branches and the polymerization rate in both the monomer-rich and the polymer-rich phase are shown. From Figure 6a, it can be seen that the polymerization rate and the net rate of formation of chloromethyl branches vary in a similar way as a function of monomer conversion in the monomer-rich phase. This is mainly due to the absence of diffusion limitations and the constant monomer concentration in this phase. Therefore, the relative importance of uni- and bimolecular reactions remains constant as a function of monomer conversion.

From Figure 6b, it can be seen that, up to the critical conversion, which is the conversion at which the monomer-rich phase disappears, the net rate of chloromethyl branch formation and the rate of polymerization vary in a similar way in the polymer-rich phase. Once the third stage of the polymerization starts, the polymerization rate decreases faster than the net rate of chloromethyl branch formation. This is mainly due to the slower decrease of the concentration of radicals leading to the formation of chloromethyl branches (i.e., radical type $R^{(3)}$) compared to the total radical concentration. The latter is explained by the absence of diffusion limitations for unimolecular reactions that lead to the formation of radicals of type $R^{(3)}$. Moreover, unimolecular reactions are not hampered by diminishing monomer concentrations at these high monomer conversions. As it is the ratio of the net rate of defect formation and the polymerization rate that determines the structural defects content, this explains why the chloromethyl content increases at higher monomer conversions.

While the increase of the chloromethyl branching content starts at the start of the third stage of the polymerization, this increase becomes only pronounced at conversions that are a lot higher than the transition conversion from the second to the third stage. This can be understood from eq 16. The content of defects at a certain polymerization time $t$is calculated as the ratio of two cumulative quantities: the

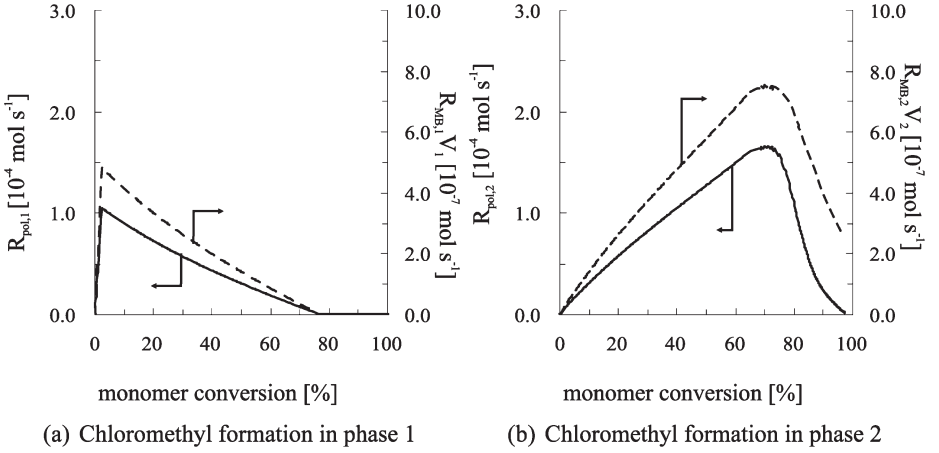

Figure 6. (Solid line) Rate of polymerization and (dashed line) net rate of formation of chloromethyl branches as a function of monomer conversion (a) in the monomer-rich phase and (b) in the polymer-rich phase.

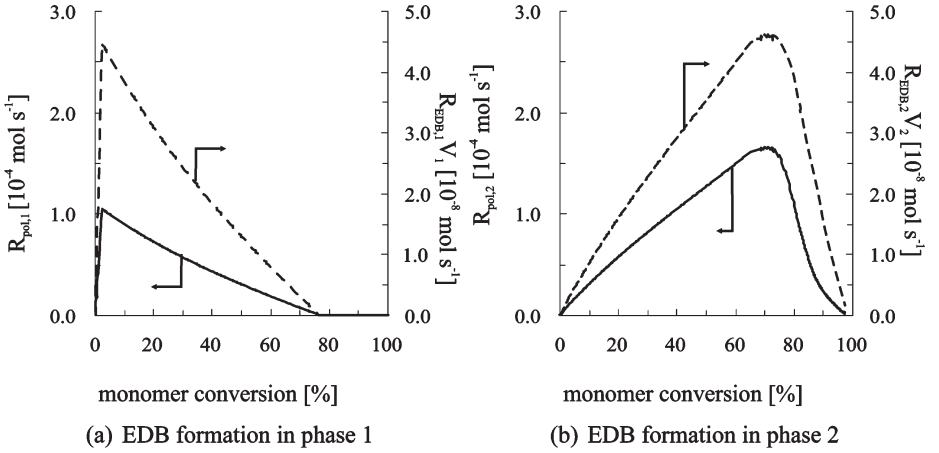

Figure 7. (Full line) Rate of polymerization and (dashed line) net rate of formation of terminal double bonds as a function of monomer conversion (a) in the monomer-rich phase and (b) in the polymer-rich phase .

Table 5. Comparison of Experimental Data on Monomer Conversion Obtained from Llauro-Darricades et al.[27] with Model Calculations[a]

			monomer conversion [%]	
no.	initiator [wt %]	batch time [h]	exp	calc
1	1	16.5	96	95.4
2	0.3	1	12	12.3
3	0.3	1.5	23	24.2
4	0.3	3.5	83	83.4
5	0.3	50	88	89.8

[a] Polymerization temperature is 328 K; initiator is dicetyl peroxydicarbonate. Calculated data obtained from integration of the equations presented in Tables S.2−S.5 with the set of intrinsic Arrhenius parameter values given in Table 4 and $f_{chem} = 1$.

number of branches formed from the start of the polymerization process until t and the total number of monomer molecules consumed by polymerization from the start of the polymerization process until time t. As the ratio of the instantaneous reaction rates only starts to vary at the start of the third stage of thepolymerization, the variation of the chloromethyl content becomes pronounced at monomer conversions that are significantly higher than the conversion indicating the transition from the second to the third stage of the polymerization.

From Figure 5c, it is clear that the content of end-of-chain-unsaturations decreases at high monomer conversions. This decrease can be explained by the consumption of these end-of-chain unsaturations by radical addition reactions. Unsaturated polymer chains can be considered macromonomers and hence react with radicals present in the reaction mixture. The relative importance of these reactions increases as the monomer concentration decreases, explaining the drop in the end-of-chain-unsaturation content at higher monomer conversions. As described in section 2.4, the rate coefficient for the addition reactions to chloroallylic end groups is 1 order of magnitude less than that of addition reactions to vinyl chloride.[9] Although one might expect on this basis that the addition to chloroallylic end groups could compete with addition to VC, the concentration of VC is several orders of magnitude larger than the concentration of chloroallylic groups. However, at high conversions, when the monomer concentration diminishes, the addition to chloroallylic end groups becomes more significant. The above argumentation is illustrated in Figure 7. Figure 7a shows the net rate of formation of terminal double bonds and the polymerization rate in the monomer-rich phase. Both rates vary in a similar way because of the constant value of the monomer concentration and the absence of diffusion limitations in the monomer-rich phase. Also, as it is assumed that polymer molecules formed in the monomer-rich phase transfer instantaneously to the polymer-rich phase, noaddition reactions to terminal double bonds can take place in the monomer-rich phase. In the polymer-rich phase, both rates vary similarly up to the start of the third stage of the

Table 6. Comparison of Experimental Data on Structural Defects Content Obtained from Llauro-Darricades et al.[27] with Model Calculations[a]

		MB [no./1000*VC*]		BB [no./1000*VC*]		EB [no./1000*VC*]		EDB [no./1000*VC*]	
no.	monomer conversion [%]	exp	calc	exp	calc	exp	calc	exp	calc
1	96	4.1	4.3	1.25	1.4	0.4	0.5	0.7	0.6
2	12	3.3	3.6	0.7	0.9	0.3	0.4	0.65	0.5
3	23	3.9	3.6	0.9	0.9	0.5	0.4	0.5	0.5
4	83	3.7	3.8	1.0	1.0	0.55	0.45	0.5	0.45
5	88	3.95	4.0	1.3	1.2	0.4	0.5	0.65	0.42

[a] Polymerization temperature is 328 K; initiator is dicetyl peroxydicarbonate. Calculated data obtained from integration of the equations presented in Tables S.2−S.5 combined with eq 16. The intrinsic Arrhenius parameter values are given in Table 4 and $f_{chem} = 1$. (MB = chloromethyl branch, BB = 2,4-dichlorobutyl branch, EB = 1,2-dichloroethyl branch, EDB = end-of-chain double bond.)

polymerization, as can be seen from Figure 7b. From the third stage of the polymerization on, the net rate of formation of terminal double bonds decreases significantly faster compared to the polymerization rate. The latter can be explained by the consumption of terminal double bonds by addition reactions. As at higher monomer conversions the monomer concentration decreases, the addition of radicals to these macromonomers becomes more important and causes the end-of-chain double bond content to decrease.

4. Validation of the Model

4.1. Monomer Conversion. Llauro-Darricades et al.[27] also performed an experimental study of PVC samples produced via suspension polymerization. The applied polymerization temperature is 328 K and the initiator dicetyl peroxydicarbonate. Table 5 presents the experimental monomer conversion and the corresponding batch times. With the presented kinetic model, the monomer conversions corresponding to the batch times given by Llauro-Darricades et al. were calculated and are shown in Table 5. A good agreement of experimental and calculated monomer conversions was obtained.

4.2. Structural Defects Content. Table 6 presents a comparison of calculated and experimental data on the structural defects content as presented by Llauro-Darricades et al.[27] All experimental data in Table 6 are obtained via ^{13}C and ^{1}H NMR. Note that no results concerning the long chain branching and the internal double bond content are presented in Table 6 as no experimental data are available for these defect structures.

From Table 6, it becomes clear that a good agreement is obtained between experimental data and model calculations. The variation of the structural defects content as a function of monomer conversion can be evaluated by comparing samples 2−5 in Table 6. Note that sample 1 corresponds to an even higher monomer conversion as compared to sample 5, but as this sample is obtained at a higher initial initiator concentration a comparison cannot be done in a straightforward manner. Similar to the profiles presented in Figure 5a, the calculated chloromethyl, 2,4-dichlorobutyl and 1,2-dichloroethyl branch content increases as a function of monomer conversion. This is in agreement with the experimentally-observed increasing chloromethyl and 2,4-dichlorobutyl branch content as a function of monomer conversion.

From Table 6, it can also be seen that the experimentally observed 1,2-dichloroethyl content first increases as a function of monomer conversion (samples 2−4) and then decreases at high monomer conversions (sample 5). This observationis in contradiction with the increase as predicted by our model calculations and as observed by Purmova et al.[9]

Furthermore, the experimental and calculated values for the end-of-chain double bond content (EDB) are also presented in Table 6. The calculated trend is similar to that presented in Figure 5c, being a rather constant value of 0.5 until a monomer conversion of 80%, after which the EDB content starts to decrease due to the consumption of terminal double bonds by addition reactions. From Table 6, it can be seen that, contrary to the work of Purmova et al.,[9] this decrease is not experimentally observed at high monomer conversions. An explanation for this discrepancy might be found in the different analytical technique used to determine the end-of-chain double bond content. In the work of Llauro-Darricades et al.[27] the number of end-of-chain unsaturations is not directly obtained by NMR, as was done by Purmova et al., but by comparison of NMR data and molecular weight data.

It is important to note that the increase in the structural defects content at high monomer conversions plays an important role toward the thermal stability of the polymer. Since the concentration of internal unsaturated structures and butyl and long chain branches increases, the concentration of allylic and tertiary chlorine also increases, hence resulting in more potential initiation sites for thermal degradation reactions. Therefore, when allowing the polymerization process to proceed until very high conversions, a PVC product will be obtained that will degrade more easily during the further processing of the product.

5. Conclusions

The free radical suspension polymerization of vinyl chloride can be modeled at the elementary reaction level, systematically taking into account diffusion limitations. It has been shown that the resulting kinetic model enables the quantitative description of conversion, averages of the molar mass distribution and the formation of structural defects as a function of polymerization time for industrially relevant conditions. By deriving balances for seven structurally distinct radical species, the formation of chloromethyl, 2,4-dichlorobutyl, 1,2-dichloroethyl, and long chain branches and of internal and terminal double bonds can be determined. Structural defects are predominantly formed at high monomer conversions. At these higher conversions monomolecular reactions, which lead to structural defects, are favored above bimolecular reactions since the latter are hampered by both diffusion limitations and lower monomer concentrations.

Acknowledgment. J.W. is a postdoctoral researcher of the Fund for Scientific Research-Flanders (F.W.O.-Vlaanderen). The Belgian Government (IAP/IUAP/PAI P6/27: "Functional Supramolecular Systems") is acknowledged for financial support.

Notation

Roman Symbols

Cl_k	Cl radical concentration in phase k ($k = 1, 2$) [mol m^{-3}]
f_k	initiator efficiency in phase k ($k = 1, 2$)
i	chain length

I_k initiator concentration in phase k ($k = 1, 2$) [mol m^{-3}]
$k_{x,k}$ apparent rate coefficient of reaction x in phase k ($k = 1, 2$) [m^3 mol^{-1}s^{-1}] or [s^{-1}]
mm_m molar mass of vinyl chloride monomer [kg mol^{-1}]
M_0 initial monomer concentration [mol m^{-3}]
M_k monomer concentration in phase k ($k = 1, 2$) [mol m^{-3}]
M_m mass averaged molar mass of polymer molecules [kg mol^{-1}]
$M_{m,k}$ mass averaged molar mass of polymer molecules in phase k [kg mol^{-1}]
M_n number-averaged molar mass of polymer molecules [kg mol^{-1}]
$M_{n,k}$ number-averaged molar mass of polymer molecules in phase k [kg mol^{-1}]
$R_{0,k}$ concentration of initiator derived radicals in phase k [mol m^{-3} s^{-1}]
$R_{MB,k}$ net rate of formation of chloromethyl branches in phase k [mol m^{-3} s^{-1}]
$R_{EB,k}$ net rate of formation of 1,2-dichloroethyl branches in phase k [mol m^{-3} s^{-1}]
$R_{BB,k}$ net rate of formation of 2,4-dichlorobutyl branches in phase k [mol m^{-3} s^{-1}]
$R_{LCB1,2}$ net rate of formation of type 1 long chain branches in phase 2 [mol m^{-3} s^{-1}]
$R_{LCB2,2}$ net rate of formation of type 2 long chain branches in phase 2 [mol m^{-3} s^{-1}]
$R_{DB,2}^{int}$ net rate of formation of internal double bonds in phase 2 [mol m^{-3} s^{-1}]
$R_{DB,k}^{end}$ net rate of formation of end-of-chain double bonds in phase k [mol m^{-3} s^{-1}]
$R_{i,k}^{(s)}$ concentration of macroradical of type s with chain length i in phase k ($k = 1, 2$) [mol m^{-3}]
$R_{pol,k}^{V}$ rate of polymerization in phase k [mol m^{-3} s^{-1}]
$P_{i,k}^{sat}$ concentration of saturated polymer molecules with chain length i in phase k [mol m^{-3}]
$P_{i,k}^{=,end}$ concentration of polymer molecules with chain length i in phase k containing a terminal double bond [mol m^{-3}]
$P_{i,k}^{=,int}$ concentration of polymer molecules with chain length i in phase k containing an internal double bond [mol m^{-3}]
t polymerization time [s]
T temperature [K] V_k
V_k volume of phase k [m^3]
X monomer conversion [−]

Greek Symbols

$\lambda_{a,k}^{(s)}$ ath order moment of the distribution of macroradicals of type s ($a = 0, ..., 2$; $s = 1, ..., 7$) [mol m^{-3}]
$\mu_{a,k}$ ath order moment of the overall polymer molecule distribution ($a = 0, ..., 2$) [mol m^{-3}]
$\mu_{a,k}^{sat}$ ath order moment of the distribution of saturated polymer molecules ($a = 0, ..., 2$) [mol m^{-3}]
$\mu_{a,k}^{=,end}$ ath order moment of the distribution of polymer molecules containing terminal double bonds ($a = 0, ..., 2$) [mol m^{-3}]
$\mu_{a,k}^{=,int}$ ath order moment of the distribution of polymer molecules containing internal double bonds ($a = 0, ..., 2$) [mol m^{-3}]
ρ_{MB} chloromethyl branching content
ρ_{EB} 1,2-dichloroethyl branching content
ρ_{BB} 2,4-dichlorobutyl branching content
ρ_{LCB1} type 1 long chain branching content
ρ_{LCB2} type 2 long chain branching content
ρ_{DB}^{int} internal double bond content
ρ_{DB}^{end} end-of-chain double bond content
$\omega_{pol,k}$ mass fraction of monomer consumed by polymerization in phase k ($k = 1, 2$)

Subscripts

k polymerization phase ($k = 1, 2$)
app apparent
chem intrinsic
diff diffusion
m monomer
p polymer, propagation
r reactor
w water

Superscripts

s radical type ($s = 1, ..., 7$)
i chain length
j chain length

Abbreviations and Acronyms

AC allylic chlorine
BB 2,4-dichlorobutyl branch
EDB end-of-chain unsaturation
EB 1,2-dichloroethyl branch
IDB internal double bond
LCB long chain branch
MB chloromethyl branch
MMD molar mass distribution
PVC poly(vinyl chloride)
TBPD *tert*-butyl peroxyneodecanoate
TC tertiary chlorine
VC vinyl chloride

Supporting Information Available: Text giving a detailed description of the considered reaction types (cf. section 2), the calculation of the structural defects content (cf. section 3) and the continuity and moment equations, a figure showing an overview of the considered elementary reactions, and tables of structure-reaction relations, mass balances for the different components, and 0th-, 1st-, and 2nd-order moment equations of the considered radical types and polymer molecules. This material is available free of charge via the Internet at http://pubs.acs.org.

References and Notes

(1) Hjertberg, T.; Sörvik, E. M. J. *Macromol. Sci.—Chem.* **1982**, *A17*, 983–1004.
(2) Hjertberg, T. Ph.D. Thesis, Chalmers University of Technology: Götenburg, Sweden, **1982**.
(3) Hjertberg, T.; Sörvik, E. M. *Polymer* **1983**, *24*, 673–684.
(4) Hjertberg, T.; Sörvik, E. M. *Polymer* **1983**, *24*, 685–692.
(5) van den Heuvel, C. J. M.; Weber, A. J. M. *Makromol. Chem. Rapid* **1983**, *184*, 2261–2273.
(6) Guyot, A. *Pure Appl. Chem.* **1985**, *57*, 833–844.
(7) Martínez, G.; Mijangos, C.; Millán, J. *Eur. Polym. J.* **1985**, *21*, 387–391.
(8) Xie, T. Y.; Hamielec, A. E.; Rogestedt, M.; Hjertberg, T. *Polymer* **1994**, *35*, 1526–1534.
(9) Purmova, J.; Pauwels, K. F. D.; van Zoelen, W.; Vorenkamp, E. J.; Schouten, A. J.; Coote, M. L. *Macromolecules* **2005**, *38*, 6352–6366.

(10) Purmova, J.; Pauwels, K. F. D.; Agostini, M.; Bruinsma, M.; Vorenkamp, E. J.; Schouten, A. J.; Coote, M. L. *Macromolecules* **2008**, *41*, 5527–5539.
(11) Starnes, W. H. J., Jr. *Polym. Sci. Polym. Chem.* **2005**, *43*, 2451–2467.
(12) Endo, K. *Prog. Polym. Sci.* **2002**, *27*, 2021–2054.
(13) Luo, Y.-R. *Handbook of bond dissociation energies in organic compounds*; CRC Press: New York, 2003.
(14) Xie, T. Y.; Hamielec, A. E.; Wood, P. E.; Woods, D. R. *Polymer* **1991**, *32*, 537–557.
(15) Xie, T. Y.; Hamielec, A. E.; Wood, P. E.; Woods, D. R. J. *Vin. Tech.* **1991**, *13*, 2–25.
(16) Kiparissides, C.; Daskalakis, G.; Achilias, D. S.; Sidiropoulou, E. *Ind. Eng. Chem. Res.* **1997**, *36*, 1253–1267.
(17) Talamini, G.; Kerr, J.; Visentini, A. *Polymer* **1998**, *39*, 4379–4384.
(18) Talamini, G.; Visentini, A.; Kerr, J. *Polymer* **1998**, *39*, 1879–1891.
(19) De Roo, T.; Heynderickx, G. J.; Marin, G. B. *Macromol. Symp.* **2004**, *206*, 215–228.
(20) De Roo, T.; Wieme, J.; Heynderickx, G. J.; Marin, G. B. *Polymer* **2005**, *46*, 8340–8354.
(21) Krallis, A.; Kotoulas, C.; Papadopoulos, S.; Kiparissides, C.; Bousquet, J.; Bonardi, C. *Ind. Eng. Chem. Res.* **2004**, *43*, 6382–6399.
(22) Wieme, J.; Marin, G. B.; Reyniers, M.-F. *Chem. Eng. Sci.* **2007**, *62*, 5300–5303.
(23) Starnes, W. H., Jr.; Schilling, F. C.; Plitz, I. M.; Cais, R. E.; Freed, D. J.; Hartless, R. L.; Bovey, F. A. *Macromolecules* **1983**, *16*, 790–807.
(24) Van Cauter, K.; Van den Bossche, B. J.; Van Speybroeck, V.; Waroquier, M. *Macromolecules* **2007**, *40*, 1321–1331.
(25) Starnes, W. H., Jr.; Wojciechowski, B. J.; Velazquez, A.; Benedikt, G. M. *Macromolecules* **1992**, *25*, 3638–3641.
(26) Starnes, W. H., Jr.; Wojciechowski, B. J. *Makromol. Chem.—Mol. Symp.* **1993**, *70/71*, 1–11.
(27) Lauro-Darricades, M.-F.; Bensemra, N.; Guyot, A.; Petiaud, R. *Makromol. Chem.—Mol. Symp.* **1989**, *29*, 171–184.
(28) Starnes, W. H., Jr.; Zaikov, V. G.; Chung, H. T.; Wojciechowski, B. J.; Tran, H. V.; Saylor, K.; Benedikt, G. M. *Macromolecules* **1998**, *31*, 1508–1517.
(29) Starnes, W. H., Jr.; Schilling, F. C.; Abbas, K. B.; Bovey, F. A. *Macromolecules* **1979**, *12*, 556–562.
(30) Rigo, A.; Palma, G.; Talamini, G. *Makromol. Chem.* **1972**, *153*, 219–228.
(31) Starnes, W. H., Jr.; Schilling, F. C.; Plitz, I. M.; Cais, R. E.; Bovey, F. A. *Polym. Bull.* **1981**, *4*, 555–562.
(32) Starnes, W. H., Jr.; Wojciechowski, B. J.; Chung, H.; Benedikt, G. M.; Park, G. S.; Saremi, A. H. *Macromolecules* **1995**, *28*, 945–949.
(33) Starnes, W. H., Jr.; Chung, H.; Wojciechowski, B. J.; Skillicorn, D. E.; Benedikt, G. M. *Adv. Chem. Ser.* **1996**, *249*, 3–18.
(34) Wieme, J.; D'hooge, D. R.; Reyniers, M.-F.; Marin, G. B. *Macromol. React. Eng.* **2009**, *3*, 16–35.
(35) Russell, G. T.; Gilbert, R. G.; Napper, D. H. *Macromolecules* **1992**, *25*, 2459–2469.
(36) Monteiro, M. J.; Subramaniam, N.; Taylor, J. R.; Pham, B. T. T.; Tonge, M. P.; Gilbert, R. G. *Polymer* **2001**, *42*, 2403–2411.
(37) Petzold, L. R. *SIAM J. Sci. Stat. Comp.* **1983**, *4*, 136–148.
(38) D'hooge, D. R.; Reyniers, M.-F.; Marin, G. B. *Macromol. React. Eng.* **2009**, *3*, 185–209.
(39) Smoluchowski, M. *Z. Phys. Chem.* **1917**, *92*, 129–168.
(40) Kruse, T. M.; Woo, O. S.; Broadbelt, L. J. *Chem. Eng. Sci.* **2001**, *56*, 971–979.
(41) Pauwels, K. F. D. Ph.D. Thesis, University of Groningen, **2004**.
(42) Park, G. S.; Saleem, M. *Polym. Bull.* **1979**, *1*, 409–413.
(43) Hjertberg, T.; Sörvik, E. M. *ACS Symp. Ser.* **1985**, *280*, 259–284.